http://dx.doi.org/10.18623/rvd.v23.4911

SIMULATION EXPLORATION OF THE IMPACT OF InGaAsP MQW AND DBR PARAMETERS DESIGN FOR ENHANCEMENT VCSEL EMITTING LASER

ANÁLISE POR SIMULAÇÃO DO IMPACTO DO PROJETO DOS PARÂMETROS DE MQW E DBR DE InGaAsP PARA O APROVEITAMENTO DO LASER DE EMISSÃO VCSEL

Article received on: 11/10/2025
Article accepted on: 2/6/2026

Lyakout Achour*
*University of Bejaia, Faculty of Technology, LMER Laboratory, Bejaia, Algeria
Orcid: https://orcid.org/0000-0001-7603-8505
lyakout.achour@univ-bejaia.dz

Lynda Benbahouche**
**UFAS, Setif1 University, Faculty of Technology, LSI Laboratory, Setif, Algeria
Orcid: https://orcid.org/0000-0001-7643-8699
lynda.benbahouche@univ-setif.dz

Smail Berrah*
*University of Bejaia, Faculty of Technology, LMER Laboratory, Bejaia, Algeria
Orcid: https://orcid.org/0000-0003-0511-9150
smail.berrah@univ-bejaia.dz

The authors declare that there is no conflict of interest

Abstract
The aim of this paper focuses on a numerical model working implemented in Silvaco atlas software that provides keys results to simulate optical-electrical VCSEL device characteristics. The optimization approach used for enhancing VCSEL performance based on different structure design staggered InGaAsP MQW and high index DBR mirror period as well as coupled from each other at an optical telecommunication wavelength. Our finding results reveals firstly that the developed model shows a good agreement with data available in literature, and fully fitted VCSEL model behaviour. Secondly, the uses of staggered InGaAsP MQW design with right composition of indium, design optimized parameters, material properties; improve the capturing probability of injected carriers with a narrower well, which has the effect of increasing the gain and reducing the threshold current with high emission at 1.5µm wavelength. Further, the best choice of material parameter of upper and lower DBR mirror (refractive index, period number) allows an enhancement efficiency of VCSEL device. Optimized VCSEL shows that the absorption rate and the reflectivity have a crucial role for achieving the appropriate wavelength as well as that exhibits higher reflectivity around the central

Resumo
O objetivo deste artigo centra-se em um modelo numérico implementado no software Silvaco Atlas, que fornece resultados essenciais para simular as características óptico-elétricas de dispositivos VCSEL. A abordagem de otimização utilizada para melhorar o desempenho do VCSEL baseia-se em diferentes projetos de estrutura, como o MQW escalonado de InGaAsP e o período do espelho DBR de alto índice, bem como no acoplamento entre eles em um comprimento de onda de telecomunicações ópticas. Nossos resultados revelam, em primeiro lugar, que o modelo desenvolvido apresenta boa concordância com os dados disponíveis na literatura e se ajusta perfeitamente ao comportamento do modelo VCSEL. Em segundo lugar, o uso do projeto de MQW de InGaAsP escalonado com a composição correta de índio, parâmetros de projeto otimizados e propriedades do material melhora a probabilidade de captura de portadores injetados com um poço mais estreito, o que tem o efeito de aumentar o ganho e reduzir a corrente de limiar com alta emissão no comprimento de onda de 1,5 µm. Além disso, a escolha ideal dos parâmetros dos espelhos DBR superior e inferior (índice de refração, número de períodos) permite um aumento da eficiência

wavelength due to the best index contrast between DBR successive layers and reaching the emission threshold.

Keywords: VCSEL Laser. Hetero-Structure. Ingaasp MQW. DBR Mirror Period. Silvaco Atlas Tool.

do dispositivo VCSEL. O VCSEL otimizado demonstra que a taxa de absorção e a refletividade desempenham um papel crucial para alcançar o comprimento de onda adequado, além de apresentar maior refletividade em torno do comprimento de onda central devido ao melhor contraste de índice entre as camadas sucessivas do DBR e ao atingimento do limiar de emissão.

Palavras-chave: *Laser VCSEL. Heteroestrutura. MQW De Ingaasp. Período Do Espelho DBR. Ferramenta Silvaco Atlas.*

1 INTRODUCTION

Recently, with a great research effort devoted by technological change cover a broad field optoelectronics system, VCSEL structures have emerged in the category of semiconductor lasers and become a key and serious candidate over the years for many range of applications, namely (disc player, blue-ray DVD, telecommunications, etc.), in the medical field (microsurgery, eye surgery), in industry (laser cutting). Also more, VCSELs currently found application in a wide range of optical systems, ranging from high-power high quality laser sources, sensing, ultrafast photonics, data storage, microwave photonics, in applications such as inertial navigation and in the high-potential space domain (satellite positioning) [Valle, A., Gymez-Molina, M., Pesquera, L. 2008], [Piprek, J., Mehta, M., Jayaraman, V. 2004], [Keever, M. 2006].

VCSEL attraction is due to numerous major advantages such as the low power consumption, circular output beam, their compactness and low production cost compared to conventional emitting lasers [Khan, Z., Chang, Y.H., Pan, T.L., Lee, C.H., Shi, J.W. 2021]. The main challenge in developing VCSELS is the simultaneous demonstration of high temperature, high speed and high power fundamental mode lasing [Uhlig, L., Washs, M., Kunzmann, D.J. 2020], [Cheng, H.T., Yang, Y.C., Liu, T.H. 2022], [Xu, L., Patel, D., Menoni, C.S. 2012], [Safaisini, R., Szczerba, K., Haglund, E. 2013]. Subsequently, the optimization of its numerous advantages is necessary, taking into account the significant technological progress in production and manufacturing. Moreover and with the development of microelectronic and optoelectronic devices, III-V, binary, ternary and

quaternary semiconductor materials [Nishida, T., Takaya, M., S. Kakinuma, S. 2005], [Vurgaftman, I., Meyer, J. R., Ram-Mohan, L. R. 2001] offer a wide variety of electronic and optical properties to choose particular technological applications [Faez, R., Marjani, A., Marjani, S. 2011], [Chaqmaqchee, F. A. I. 2014], [Sarzala, R., Czyszanowski, T., Wasiak, M. 2012].

The first continuous emission VCSEL based on the GaAs system using metallic and dielectric mirrors took place in the late 1980s [F. Koyama, S. Kinoshita, and K. Iga, 1989]. Over the years, this technology is the most mature VCSEL technology both for research and for data manufacturers. However, heating during device operation is one of the factors limiting its performance, which generally due to the design (materials, geometry) and the confinement method used.

As reported by [K. L. Lear *et al*., 1997], the use of an active region made up of multi-unconstrained GaAs/AlGaAs quantum wells leading to a bandwidth greater than 20 GHz but unfortunately limited by thermal effects. However, T. Aggerstam and al. [T. Aggerstam, R. M. von Wurtemberg, C. Runnstrom, and E. Choumas, 2002] investigate the use of constrained quantum wells to improve internal quantum efficiency. While S. A. Blokhin and al [S. A. Blokhin and al., 2009] are able to increase data rates reaching 40 Gbps using VCSELs emitting at 850 nm based on InGaAs quantum wells. L. Chorchos and al [L. Chorchos and al., 2019] and H.-L. Wang.al [H.-L. Wang,

W. Fu, J. Qiu, and M. Feng, 2019], studies investigate the achievement bandwidth above 50 Gbps for standardized short-distance communications. Progress continues in their expanding applications in optical communications (laser printers using 2D matrices of Xerox VCSELs [T. Kondo *et al*., 2016], [R. L. Thornton, 1997]), optical computer mice [D. Collins and N. Li, 2010], mice wireless powered by internal battery, laser autofocus for photos, photonic microwave signal generation [Althrthy, S. S. 2022]. In literature review, its integration by Apple company and especially in 2018, five new smartphones were designed with integrated 3D facial recognition modules using VCSELs and this continued during 2019 (Yole Development [VCSELs, 2019]). Indeed, according to [VCSELs, 2019] by using innovative technologies such as driver facial recognition, VCSELs are becoming very promising light sources for new generations of vehicles.

The main objective of this study is looked at challenge and a potential of VCSEL device to achieve high quantum efficiency taking into account some useful design

modeling which apply likes in the case of the optically pumped as well as the effect of MQW and DBR design on optical communication wavelength by modelling and simulation. The current research work is carried out using Matlab and Silvaco Atlas software [Silvaco, 2015], [Liu, A., Bimberg,D. ,2016] studying the dependence of active region staggered MQW designs on the electrical and optical characteristics of VCSEL studied with optimized thickness and without mitigated VCSEL efficiency. Further, our study take into account the lattice matching of materials employed in VCSEL design structure to avoid the appearance of stress and minimizing the temperature rise in the active region. We will discuss the VCSEL performance with high or low number quantum well and we will provide an understanding on efficiency limitation caused by incorporating thinner layer in the active region. Furthermore, we will discuss about the DBRs mirror effects and their quality factors such as adjustment material composition, refractive index, upper and lower period mirror design, on how the VCSEL efficiency can be further improved.

2 MODELING METHODOLOGY

The study of most semiconductors is based on the simultaneous resolution of the Poisson equation and the continuity equation in order to determine a large number of unknowns: the concentration of electrons and holes, electric field, current densities, [Moatlhodi, O., Ditshego, N. M. J. 2020], [Hong, K. B., Huang, W. T., Chung, H. C. *et al*. ,2021], [Johnson, B., Jabbour, J., Malonson, M., Mallon, E. *et al*. 2022]. These physical quantities appear in a discretized form, as a sequence of finite elements. In this step ATLAS will solve a series of equations (equation of continuity, Poisson and diffusion equation) to calculate the carrier densities, potentials and currents by using Newton method [Goyal, P., Sharma, M., Jha, A., Kumari, M., Singh, S.P., Singh, N., Kaur, G. 2016], [Yang, Y. D., Tang, M., Wang, F. L., Xiao, Z. X. *et al*. 2019].

The main models used in our simulation providing a robust framework are mathematical models including Poisson's equation, carrier continuity equation, drift-diffusion model (DDM), energy balance transfer model, concentration dependent carrier mobility. Further, Schockley-Read-Hall (SRH), Auger, and Radiative Recombination (OPTR) for optical recombination, as well as MQW models for gain

and spontaneous recombination that account for quantum carrier confinement inside of the wells. Besides, Quantum effect Simulator for determining the bound state energies (lowest bound state energy in the conduction band and the highest bound state energy in the valence band), a secondary quantum mesh must be set up for the solution of the Schrodinger's equation, allowing laser gain calculations. In addition, we use the mobility's models since they directly affect series resistance.

Additionally, the materials used in this work are carefully chosen according to their optoelectronic properties and lattice matching system. Their uses for VCSELL design can be achieve through a code model implemented in Silvaco Atlas [Silvaco, 2015]. Subsequently, the simulation and optimization of semiconductor materials used in the design of VCSEL structure will be taken into account for its optimization such as (energy gap, affinity, dielectric permittivity, carrier mobility, carrier lifetimes etc…, as well as the optical constants (n,k)). The gap and the lattice constant is calculated according to Vegard's law in order to avoid lattice mismatch between materials [Sarzala, R., Czyszanowski, T., Wasiak, M. 2012], [Hong, K. B., Huang, W. T., Chung, H. C. *et al*. , 2021]. Most of the parameters used to model the VCSELL device are calculated using Matlab software by varying the technological parameters likes molar fraction and /or are taken from the Sopra database [Silvaco, 2015], in order to obtain accurately parameters and to specify the best estimate.

3 VCSEL DESIGN AND IMPLANTATION

For a good, successfully design of VCSELL device and accelerate the program convergence (execution time), two main conditions are taken carefully into consideration: active region and DBRs mirror designs by choosing material parameters (bandgap, affinity, also more..), which allow to operate near the peak gain. The materials properties required are defined via the material statements as input parameters and summarizes in Table.1. Hence, we will move on the simulation of its electrical and optical characteristics. VCSELL structure studied is exposed to an ambient temperature of 300°K. Once we have ensured the implantation and validation of the developed model, the VCSEL structure studied has been simulated and the results have been discussed.

Fig.1 shows the simulated VCSEL structure design with coupled staggered multi-quantum well (MQW) active region composed of six 5.5 nm thick $In_{0.76}Ga_{0.24}As_{0.82}P_{0.18}$ quantum wells and 8 nm thick $In_{0.48}Ga_{0.52}As_{0.82}P_{0.18}$ barriers and two upper and lower DBR (Distributed Bragg reflectors) mirrors. The MQWs are embedded in InP spacer layers which have been extended by thin layers of GaAs above each a mirror to increase the emission wavelength.

Table 1

Materials parameters used in numerical calculation

Region	Materials	Parameters	Value
Substrate	n GaAs	Thickness	250µm
		Doping	1E19cm^{-3}
Bottom Contact region	n GaAs	Thickness	0,02µm
		Doping	5E18
Bottom DBR	nGaAs/nAlAs	Thickness	0.115/0.134
		Doping	1E18/1E18
		Repetition	56
Spacer	nInP/nInP	Thickness	0.05/0.258
		Doping	1E18/5E18
Active Region	InGaAsP/ InGaAsP	Thickness	0.0082/0.005
		Molar fraction x,y/xy	0.24,0.82/ 0.52,0.82
		Repetition	6W,7B
Spacer	pInP/pInP	Thickness	0.1/0.178
		Doping	1E16/1E18
Top contact Region	pGaAs/pGaAs	Thickness	0.02/0.184
		Doping	2E19/4E17
Top DBR	AlGaAs/GaAs	Thickness	0.127/0.11
		Doping	4E17/4E17
		x	0.7
		Repetition	60
Spacer	pGaAs/pGaAs	Thickness	0.02/0.01
		Doping	4E17/4E19

While the two DBR mirrors are made of alternating layers of high 3.38 and low 3.05 refractive index of *GaAs/*$Al_{0.33}Ga_{0.67}As$ form the upper 30-period p-type mirror DBR while the lower n-type DBR mirror is formed of 28 periods of *GaAs/AlAs* layers of refractive index 3.35 and 2.89 respectively. The thickness of each of their layers be

exactly a quarter of the desired laser wavelength as well as showing a good lattice matching [A. Miller, M. Ebrahimzadeh, M. Ebrahimzadeh, and D. M. Finlayson, 1999].

Figura 1

Schematic structure of VCSEL studied

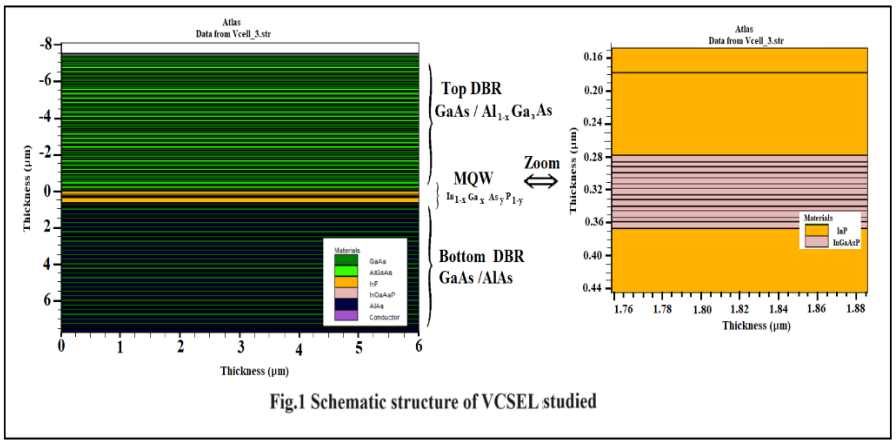

Fig.1 Schematic structure of VCSEL studied

4 RESULTS AND DISCUSSIONS

In this section, various structure designs will be presented and their effects on quantum VCSEL efficiency will be discussed in terms of maximum output power, optical emission spectra, threshold current, and absorption rate to finally recover their thermal performance in terms of lattice temperature.

4.1 Optimization of active MQW

We start with the first objective of this work by a series of simulation results to highlight the effect of the number of quantum wells (QWs) in the active region as well as we use InP/InGaAsP/InGaAsP active regions with right composition of indium designed to emit near 1.5 µm. Additionally, the same parameters like thickness, DBR period and molar fraction are maintained except by adding a well and a barrier.

Figura 2

Conduction and Valence bands of VCSEL studied

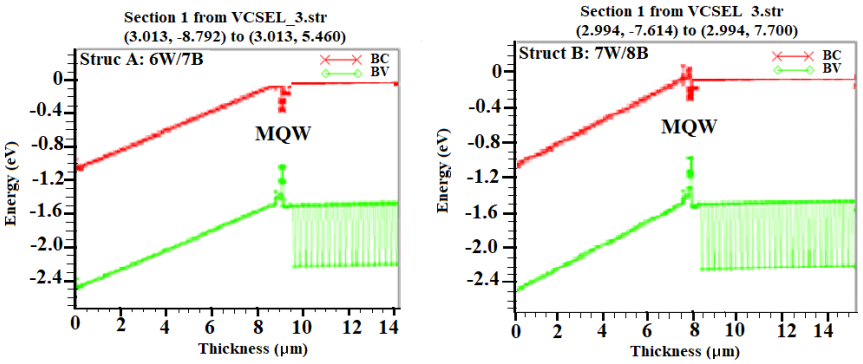

Fig.2 Conduction and Valence bands of VCSEL studied

Figura 3

I-V Characteristics of VCSEL studied

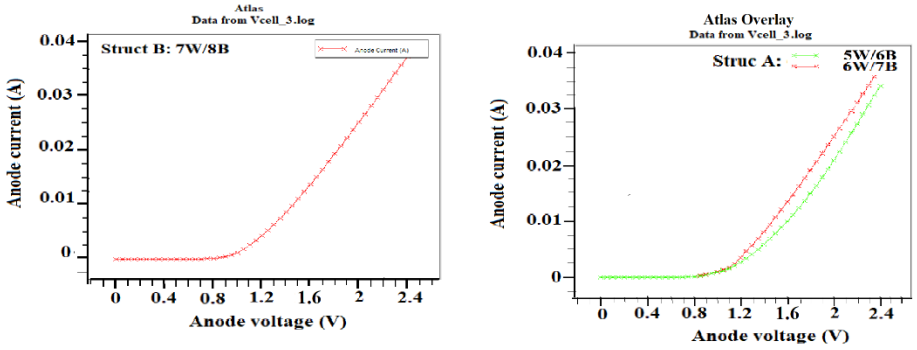

Fig.3 I-V Characteristics of VCSEL studied

By observing both I-V characteristics for 6W/7B and 7W/8B, the thickness of the MQW active region is increased which consequently reduces the rate of carrier generation rate. Similarly, a slight increase in electric current is noticed, because the quantum well barrier is thick enough (8nm) to prevent carrier tunnelling from occurring between the wells. For this purpose, each well can be treated as a separate transport tank.

Another characteristic that catches our attention is the P-I characteristic. We observe that the output optical power increases with increasing current.

Figura 4

P-I Characteristics of VCSEL studied

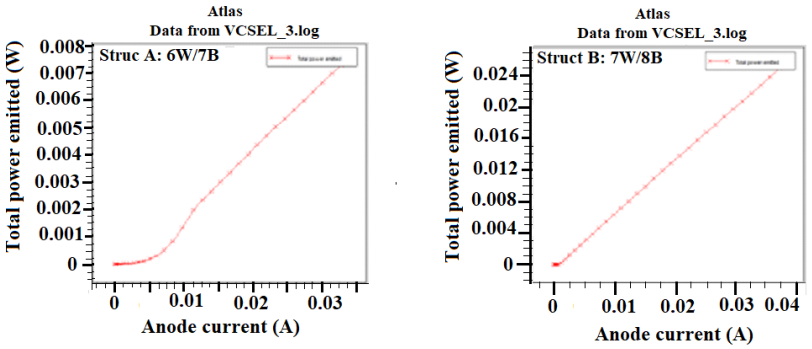

Fig.4 P-I Characteristics of VCSEL studied

The P-I characteristic depicted in Fig. 4 shows the increase in the total power emitted at higher current values as the number of W/B is increased.

In addition, the power output peak reached 25mW for 7W/8B at current of 37.4mA higher than for 6W/7B of the order of 7.2mW for a current of 37.4mA. The power of the output light follow the form that is expressed in literature by [Merwan Mokhtar, 2019]:

$$P = \eta \frac{h\nu}{q}(I - I_{th}) \qquad (1)$$

where η:

the differential quantum efficiency, hv: photon energy, q; electron charge, I: the drive current and I_{th}: the threshold current.

According to equ (1), quantum efficiencies is proportional to the optical power emitted. To this end, as the number of quantum well increases, higher optical power is observed allowing an increase in quantum efficiencies of VCSEL device.

Figura 5

P-V Characteristics of VCSEL studied

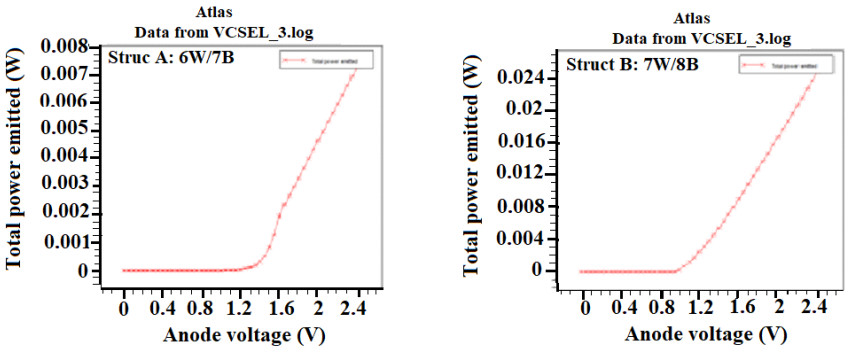

Fig.5 P-V Characteristics of VCSEL studied

By showing the P-V characteristic for the two cases studied, the peak output power reached at V=2.4V is 24mW for the case of 7W/8B, and 7.2mW for the case of 6W/7B due to the increase in the recombination rate (See Fig.6).

Figura 6

Recombination rate as function of depth of VCSEL studied

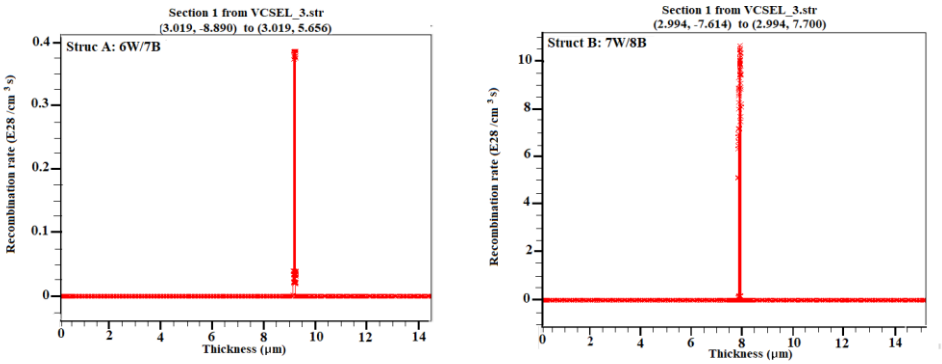

Fig.6 Recombination rate as function of depth of VCSEL studied

Based on simulation results in Fig.6, the increase of QW number provides an increase of the recombination rate, which is 1.1E29/cm^{3}s for the case 7W/8B compared for the case 6W/7B is 4E27/cm^{3}s. These results lead to produce higher photon densities, which surely contribute to the higher optical power observed at higher operating bias.

Figura 7

Gain variation as function of voltage

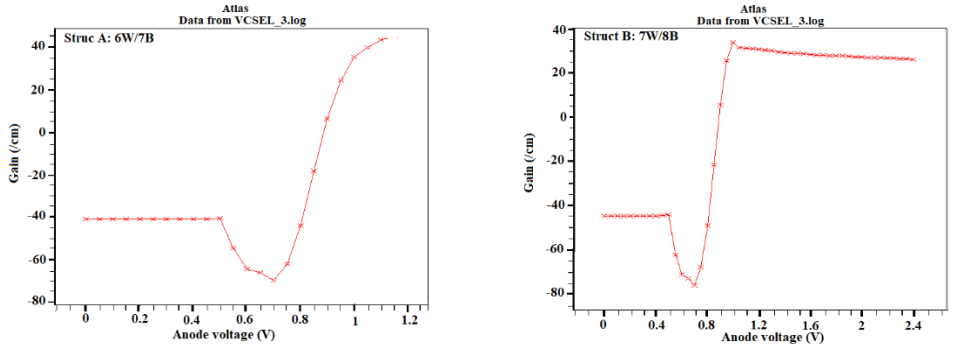

Fig.7 Gain variation as function of voltage

In both cases, we find that at voltage values below the threshold, the gain is negative, which reflects the absence of a laser emission, on the other hand at voltage values above the threshold; the gain is positive which reflects the start of a laser emission.

As deduced from gain curves shown in Fig.7, a decreasing gain value from 45.6 cm^{-1} to 33.1 cm^{-1} for case 6W/7B and 7W/8B respectively. Since the gain of the VCSEL devices strongly depends on the resonance wavelength of the cavity, the effect of the number of well/barrier will be associated to the variation of the cavity length, being able to relate fairly the optical performance of VCSEL. As resulting, the increase in QW number leads to reduce the density of states and subsequently the material gain.

When the VCSEL is forward biased, electrons and holes are injected in the active region of the device where recombination often occurs. These electrons and holes recombine to emit photons. In the same way, we will notice in the case of 7W/8B, the gain reaches the phenomenon of saturation more quickly than in the case 6W/7B.

In order to check the behaviour of the transmission modes in a VCSEL laser, these modes are activated by the statement atlas Silvaco mode=4. The variation of the gain as a function of the voltage by transmission mode for the two cases are presented in Fig.8.

Figura 8

Gain variant as function of voltage by transmission mode

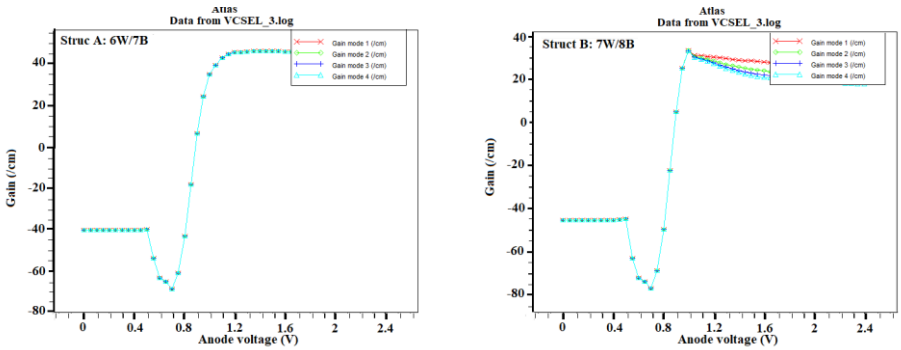

Fig.8 Gain variation as function of voltage by transmission mode

We note that below the threshold voltage, the gain is identical in the four modes for the two cases 6W/7B and 7W/8B. Above the threshold voltage, the gain for the case 6W/7B is almost identical for the four modes. On the other hand, for the case 7W/8B, a slight decrease in the gain is observed and the fundamental mode is the most effective.

Figura 9

Laser power per mirror as function of voltage by transmission mode

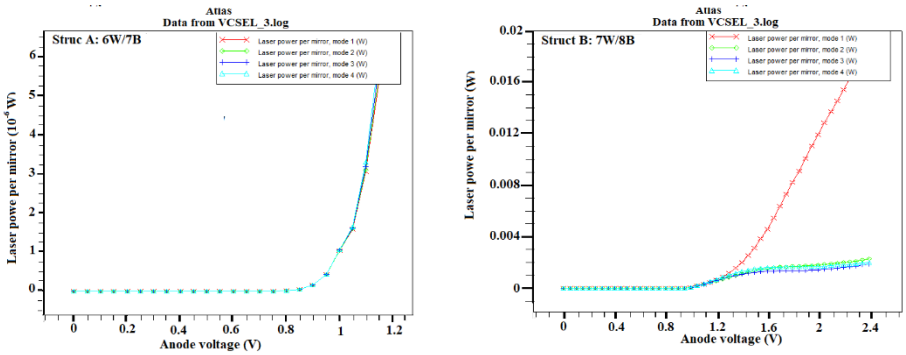

Fig.9 Laser power per mirror as function of voltage by transmission mode

As depicted in Fig.9, it can be observed that the laser power mirror emitted according to the four transmission modes are zero below the threshold voltage 0.9V, which means the absence of laser emission for both cases studied because the current fails to achieve the population inversion. In the case 6W/7B and at values greater than 0.9V, the laser power keeps the same value and the same slope, so there is only one mode. While for the case 7W/8B, the laser power per mirror for mode 1 shows a slope which increases

sharply at the higher values 18.8mW, while the other three modes the laser powers curves increase to 2.2mW.

Self-heating in VCSEL laser diodes during their use mainly affects the function of the carrier distribution and the bandgap of the semiconductors used. This leads to the degradation of its laser output performance by the presence of temperature-related resonance, wavelength shift, etc. Thus, our VCSEL studied was exposed to an outdoor temperature of 300°K.

Figura 10

Lattice temperature for both cases as function of depth

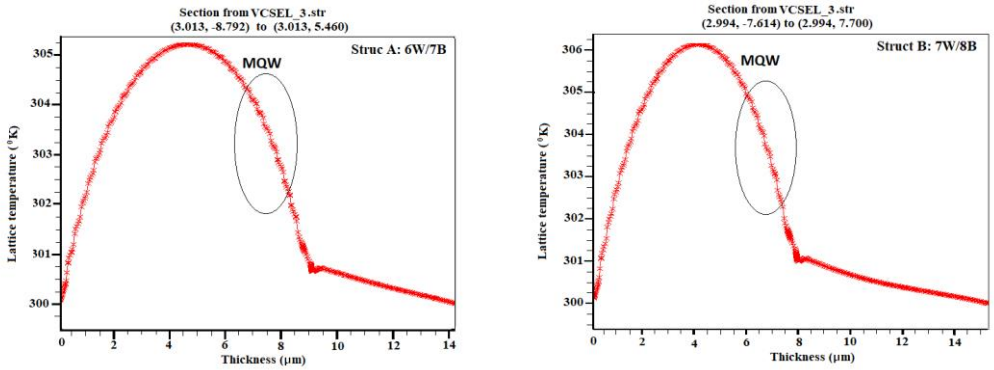

Fig.10 Lattice temperature for both cases as function of depth

We find that, for both case a decrease in temperature is pronounced in the MQW zone. This confirms the advantage of using MQWs in VCSELs to decrease temperature sensitivity [Merwan Mokhtar, 2019].

Figura 11

Global temperature as function of injected current

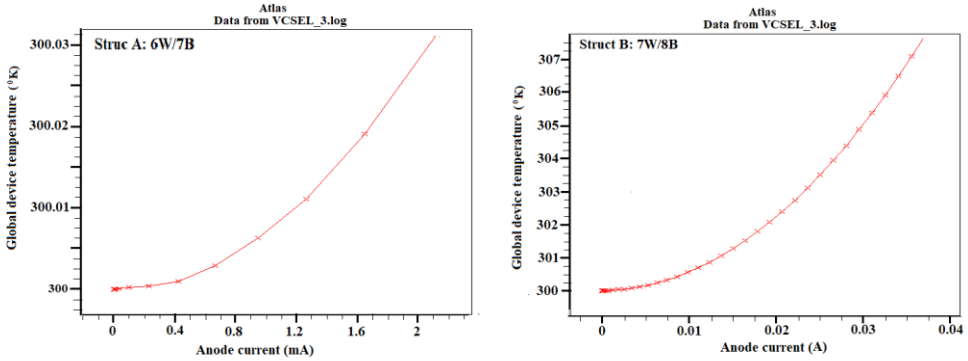

Fig.11 Global temperature as function of injected current

We observe that the global temperature increases linearly with the injection current. In the case 6W/7B, the maximum temperature is 307.7°K corresponding to an injected current of 37.25mA. Whereas for the case 7W/8B the temperature reaches 300.03°K for an injected current of 2.12mA. This supports the theory that as the number of well and barriers in the active layer increases, the temperature sensitivity decreases [Merwan Mokhtar, 2019].

Figura 12

Optical wavelength as function of injected current

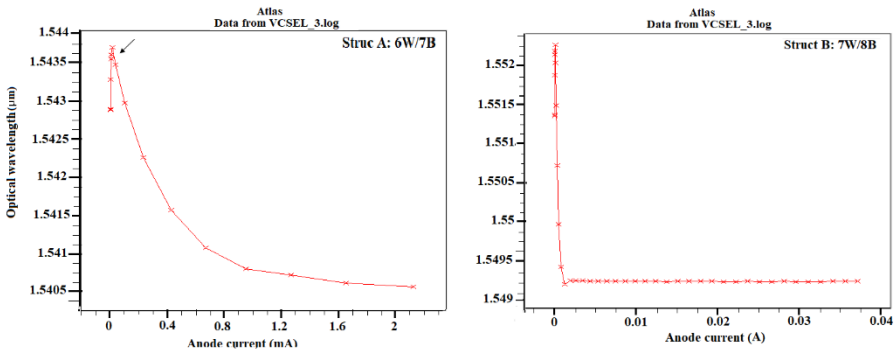

Fig.12 Optical wavelength as function of injected current

As depicted in Fig.12, for 7W/8B a narrow peaked of the optical wavelength intensity is enhanced compared to 6W/7B at the designed emission wavelength 1.5μm, which is due to the micro-cavity resonance. When the number of QW is increased, the peak resonance wavelength increases from 1.5445μm for 6W/7B to 1.5535μm for 7W/8B

at 0.1mA. We will notice that the increase in peak wavelength occurred according to the equation [Merwan Mokhtar, 2019]:

$$nL = m\frac{\lambda}{2} \quad (2)$$

where:

n is the effective refractive index of the active region, *L* is the effective region thickness, *m* is the propagation mode (in this case, m=1 for single mode operation) and λ peak of the wavelength.

4.2 Optimization DBR mirror

In this section, to identify the optimum design of the VCSEL structure which will ensure the best thermal performance, the impact of the upper (GaAs/AlGaAs) and lower (GaAs/AlAs) DBR mirror period will be evaluated in the case of VCSELs structure integrating an InP/InGaAsP/InGaAsP active region. Three cases are taken into account: first case, VCSEL design with (60periods/56 periods) for the upper/lower DBR mirror respectively, while the second case with (56periods/56 periods) and finally with (56periods/60 periods). To this purpose, we will analyze the simulation results obtained to assess the impact of these cases, which could lead to improvements in the design, and optimization of VCSELs for specific applications such as optical communication or optical sensors.

Figura 13

Reflectivity variation as function of energy

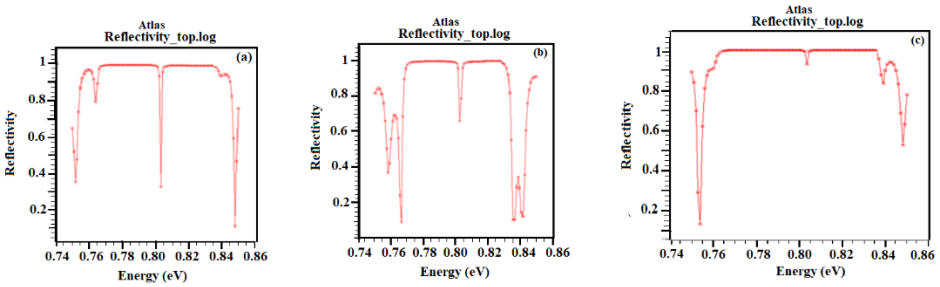

Fig.13 Reflectivity variation as function of energy

As depicted in Fig.13, we can clearly see that the value of the reflectivity corresponding to the energy of the photon of 0.8eV is better in the third case 28/30 DBR period where we record a value of 0.93 of reflectivity. Further, we can notice that the maximum reflectivity value can be reached with a limitation of DBR period when a good choice of refractive index.

Figura 14

Absorption variation as function of energy

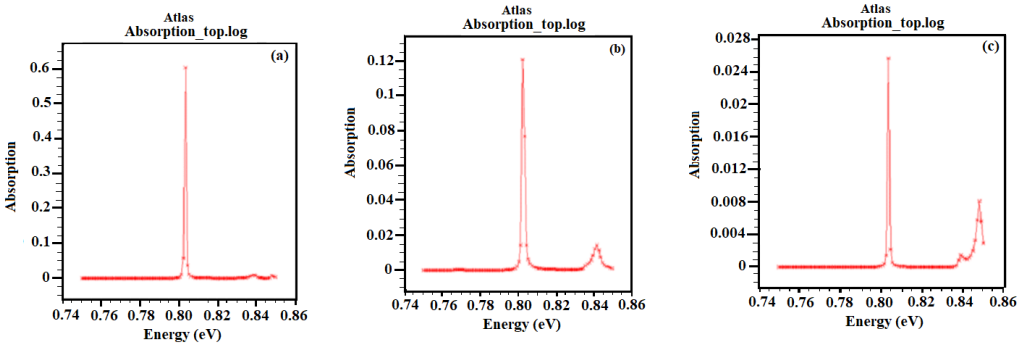

Fig.14 Absorption variation as function of energy

According to Fig.14, the absorption is minimal in the third case (c), so our structure is better because most of the energy produced is exploited.

The result of simulations clearly show that with a greater number of DBR period that resulting thicker and poorly conductive structures, we can compensate the using a lower index contrast. Subsequently, an increase of laser threshold is observed allowing limit of output power that reduce DBRs performance for the VCSEL devices. In

opposition, the use the materials DBR with higher refractive index contrast allow to achieve a high reflectivity value and then compensating the cavity losses.

Furthermore, as reported in literature, the resonant configuration allows to a higher gain which results in a lower threshold at the designed emission wavelength. This configuration as knowing gets to reach laser oscillation of VCSEL studied when changing the thickness of the sub-cavity [A. Miller, M. Ebrahimzadeh, M. Ebrahimzadeh, and D. M. Finlayson, 1999].

5 CONCLUSIONS

The main challenge of this paper is to study the effect of the promising design optimization of VCSEL laser device and to overcome the problem of their designs that remain very expensive, by simulation. In this context, our objective is the modeling, simulation and electrical-optical characterization of a VCSELL device that is more used in our daily lives through various applications by using Silvaco Atlas software. This later incorporates an active cavity consisting of multi-quantum wells (MQW) based on the quaternary compound InGaAsP/InP, two DBR reflecting mirrors in the vertical direction composed of stacks of low and high index of alternating reflections where the thickness of each of the layers be exactly a quarter of the desired laser wavelength in the component.

Our simulation results allowed us to take some characteristics of the VCSEL and analyze their behavior during laser transmission. We start with the first objective of this work by a series of simulation results to highlight the effect of the number of quantum wells (QWs) in the active region as well as we use staggered MQW InP/$In_{0.76}Ga_{0.24}As_{0.82}P_{0.18}$ /$In_{0.48}$ $Ga_{0.52}As_{0.82}$ $P_{0.18}$ with right composition of indium, improve the capturing probability of injected carriers with a narrower well.

As results of the advantages offered by MQW in terms of lower threshold current, output optical power, the modal gain, global temperature, lattice temperature, peak resonance wavelength and less temperature sensitivity have a profound effect on VCSEL performance characteristics. Moreover, the VCSEL studied emits several modes of transmission but only the fundamental mode is effective.

Furthermore, after in-depth analysis, we concluded that DBR mirror in terms of refractive index for material used and DBR period can be lead to improve the overall

performance of the VCSEL laser device and to reach the specific telecommunications windows. As observed, VCSEL with an increase of DBR period number can compensate the using a lower index contrast. Subsequently, the thicker structure allows to an increase of laser threshold that forcedly limit the output power that reduce DBRs performance for the VCSEL devices. In opposition, the use the materials DBR with higher refractive index contrast allow to achieve a high reflectivity value and then compensating the cavity losses.

In summary, our analysis highlighted the importance of the active layer and quantum wells in the operation of VCSEL. By adjusting the number of quantum wells, we optimize the laser performance in terms of quantum efficiency, current and power.

ACKNOWLEDGEMENTS

This work is supported by the General Directorate of Scientific Research and Technological Development, Ministry of Higher Education and Scientific Research and LMER Laboratory, Faculty of Technology, Bejaia University, Bejaia, 06000, Algeria.

REFERENCES

Chaqmaqchee, F. A. I. Optically and electrically pumped ga0.65in0.35n0.02as0.98/gaas vertical-cavity surface-emitting lasers (VCSELs) for 1.3 μm wavelength operation. *Arabian journal for science and engineering*, v. 39, p. 5785–5790, 2014. http://dx.org/10.1007/s13369-014-1126-3

Cheng, H. T.; Yang, Y. C.; Liu, T. H. Recent advances in 850 nm VCSELs for high-speed interconnects. *Photonics*, v. 9, p. 107–133, 2022. https://doi.org/10.3390/photonics9020107

Faez, R.; Marjani, A.; Marjani, S. Design and simulation of high power single mode 1550 nm Ingaasp VCSELs. *Ieice electronics express*, v. 8, p. 1096–1101, 2011. http://doi.org/10.1587/elex.8.1096

Keever, M. Avago technologies VCSEL design and integration. *Iii-vs review the advanced semiconductor magazine*, v. 19, p. 32–34, 2006. https://doi.org/10.1016/S0961-1290(06)71767-7

Khan, Z.; Chang, Y. H.; Pan, T. L.; Lee, C. H.; Shi, J. W. High-brightness, high-speed and low noise VCSEL arrays for optical wireless communication. *Ieee access*, v. 10, p. 2303–2317, 2021. http://doi.org/10.1109/ACCESS.2021.3133436

Nishida, T.; Takaya, M.; Kakinuma, S. 4.2-mw gainnas long-wavelength VCSEL grown by metalorganic chemical vapor deposition. *Ieee journal of selected topics in quantum electronics*, v. 11, p. 958–961, 2005. http://doi.org/10.1109/JSTQE.2005.853734

Piprek, J.; Mehta, M.; Jayaraman, V. Design and optimisation of high performance 1.3 µm VCSELs. *Physics and simulation of optoelectronic devices xii*, v. 5349, p. 375–384, 2004. http://doi.org/10.1117/12.543062

Safaisini, R.; Szczerba, K.; Haglund, E. 22 gb/s error-free data transmission beyond 1 km of multi-mode fiber using 850 nm VCSELs. *Proceedings of spie*, v. 8639, 2013. http://dx.doi.org/10.1117/12.2003693

Sarzala, R.; Czyszanowski, T.; Wasiak, M. Numerical self-consistent analysis of VCSELs. *Advances in optical technologies*, 2012. http://doi.org/10.1155/2012/689519

Uhlig, L.; Washus, M.; Kunzmann, D. J. Spectral-temporal dynamics of (Al,In)gan laser diodes. *Optics express*, v. 28, p. 1771–1789, 2020. https://doi.org/10.1364/OE.382257

Valle, A.; Gymez-Molina, M.; Pesquera, L. Polarisation bistability in 1550 nm wavelength single mode VCSEL subject to orthogonal optical injection. *Ieee journal of selected topics in quantum electronics*, v. 14, p. 895–902, 2008. http://doi.org/10.1109/JSTQE.2008.918044

Vurgaftman, I.; Meyer, J. R.; Ram-mohan, L. R. Band parameters for iii-v compound semiconductors and their alloys. *Journal of applied physics*, v. 89, p. 5815–5875, 2001. http://dx.doi.org/10.1063/1.1368156

Xu, L.; Patel, D.; Menoni, C. S. Carrier recombination dynamics investigations of strain-compensated Ingaasn quantum wells. *Ieee photonics journal*, v. 4, p. 2382–2389, 2012.

Authors' Contribution

All authors contributed equally to the development of this article.

Data availability

All datasets relevant to this study's findings are fully available within the article.

How to cite this article (APA)

Achour, L., Benbahouche, L., & Berrah, S. SIMULATION EXPLORATION OF THE IMPACT OF InGaAsP MQW AND DBR PARAMETERS DESIGN FOR

ENHANCEMENT VCSEL EMITTING LASER. *Veredas Do Direito*, e234911. https://doi.org/10.18623/rvd.v23.4911